Diagnosing pure-electron plasmas with internal particle flux probes

J. P. Kremer, T. Sunn Pedersen, Q. Marksteiner, R. G. Lefrancois, and M. Hahn
Applied Physics and Applied Mathematics Department, Columbia University, New York, New York 10027

(Received 13 October 2006; accepted 9 December 2006; published online 22 January 2007)

Techniques for measuring local plasma potential, density, and temperature of pure-electron plasmas using emissive and Langmuir probes are described. The plasma potential is measured as the least negative potential at which a hot tungsten filament emits electrons. Temperature is measured, as is commonly done in quasineutral plasmas, through the interpretation of a Langmuir probe current-voltage characteristic. Due to the lack of ion-saturation current, the density must also be measured through the interpretation of this characteristic thereby greatly complicating the measurement. Measurements are further complicated by low densities, low cross field transport rates, and large flows typical of pure-electron plasmas. This article describes the use of these techniques on pure-electron plasmas in the Columbia Non-neutral Torus (CNT) stellarator. Measured values for present baseline experimental parameters in CNT are $\phi_p=-200\pm2$ V, $T_e=4\pm1$ eV, and n_e on the order of 10^{12} m^{-3} in the interior. © *2007 American Institute of Physics.*
[DOI: 10.1063/1.2431084]

I. INTRODUCTION

Much of the study of pure-electron plasmas has been conducted in Penning-Malmberg traps[1–3] and partial toroidal traps.[4] The open field lines of these configurations allow for relatively simple yet powerful diagnostics such as phosphor screens,[5,6] Faraday cups,[7] and energy analyzers.[5,8] In closed field line configurations such as complete pure toroidal traps[9–11] and magnetic surface configurations,[12–14] these diagnostics cannot be used. The low density and relatively low temperatures of electron plasmas would result in unacceptably low signal-to-noise ratios using diagnostics often employed in quasineutral fusion plasmas (e.g., Thomson scattering, etc.). Therefore, these diagnostics may be difficult or impossible to use on electron plasmas. Their simplicity and low cost make particle flux probes an attractive choice for toroidal magnetically confined pure-electron plasmas.

The equilibrium of pure-electron plasmas on magnetic surfaces is characterized by potential, density, and temperature.[12] Each of these can, in many situations, be measured through the use of emissive and Langmuir probes. Experimental exploration and confirmation of theoretical equilibrium predictions[12] rely heavily on the ability to measure all three parameters well. Such experiments have been successfully performed in the Columbia Non-neutral Torus (CNT)[15] using the methods described here.

In this article, the use of emissive and Langmuir probes to measure plasma potential, density, and temperature is described. Complications arising from the low densities, low cross field transport rates, and large flows typically associated with pure-electron plasmas will be discussed as will methods employed to make measurements possible in spite of such complications. This article is arranged as follows. The experimental apparatus will be introduced in Sec. II. In Sec. III, aspects of Langmuir and emissive probe theory pertaining to the measurement of local plasma potential (floating potential measurements and the so-called "deviation potential"), electron density, and temperature will be discussed. A detailed description of how these theories were applied to actual measurements in the Columbia Non-neutral Torus (CNT) stellarator will be described in Sec. IV. This article is then summarized in Sec. V.

II. APPARATUS

A. The CNT device

Stellarators differ from tokamaks in that the magnetic topology is created from external coils; no plasma current is needed to create the magnetic surfaces.[16,17] The CNT is the first stellarator designed to study pure-electron, partially neutralized, and electron-positron plasmas on magnetic surfaces. Stellarators are, like tokamaks, toroidal configurations of nested magnetic surfaces. Pure-electron plasmas are currently being studied. CNT is a small university-scale stellarator created from only four circular, planar coils. Two are interlocking and reside inside the large vacuum chamber, and the other two form a Helmholtz coil set which resides outside the vacuum chamber. The major radius of the confining region is $R\approx30$ while the minor radius is $a\approx15$ cm. The magnetic field can be varied from $B=0.004$ to $B=0.03$ T but experiments described in this article were all performed at $B=0.02$ T. The neutral pressure for these experiments was $p_n\approx2\times10^{-8}$ Torr. The ion fraction typical of such neutral pressures was measured to be $\leq1\%$ through the measurement of the ion-saturation current of a probe large enough to collect a measurable ion current. A computer aided design (CAD) cut-away drawing of CNT device is shown in Fig. 1. A detailed description of the CNT device can be found in other publications.[12,15,18–20]

B. Electron Injection

Electrons are injected from a single heated, biased, thoriated tungsten filament placed in the confining region. The

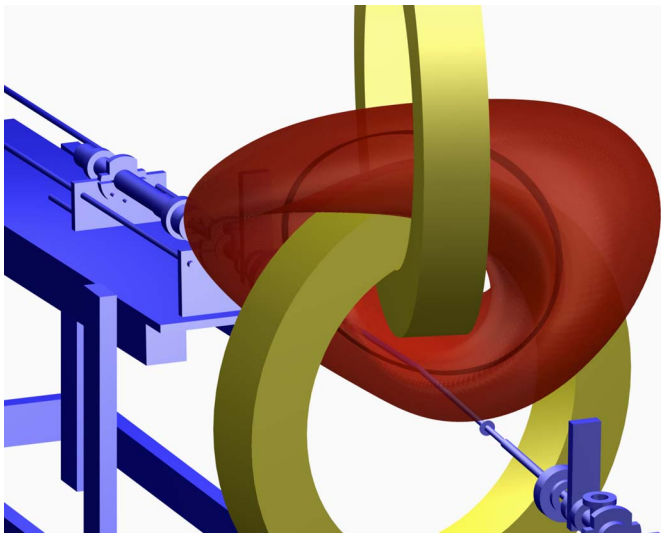

FIG. 1. (Color online) A cut-away drawing of the CNT device. The interlocking coils are shown in yellow and the confining volume in red. The emitter and diagnostic rods with their supporting tables are shown in blue. The electron emitter rod is positioned such that the emitter is placed on the magnetic axis (dark red).

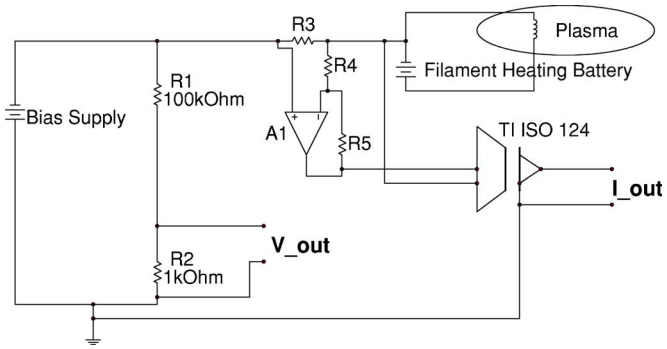

FIG. 2. (Color online) A schematic of the emitter and probe filament potential and current measurement circuit. The filament potential is measured across a voltage divider made from R_1 and R_2 (V_{out}) while the current to the filament is measured as the voltage across R_3. This is shown as I_{out} in the schematic. The large common-mode voltage of R_3 with respect to ground necessitates the use of an isolation amplifier (a TI ISO-124) to translate the voltage across R_3 to a voltage with respect to ground. The A_1 amplifier, with R_4 and R_5, acts as a buffer between the high impedance of R_3 and the high input impedance of the isolation amplifier.

filaments used are 10 W halogen light bulbs with the bulb glass removed. These filaments are tightly spiral-wound to form a cylinder with diameter $d \approx 1$ mm and length $L \approx 4$ mm. A 6 V battery is used to supply the filament heating current.

To emit electrons, a negative bias relative to ground (i.e., the vacuum chamber) is applied to the heated emitting filament. A current of electrons, $I_{emission}$, from the emitter quickly fills the surface that intersects the filament. Cross field transport then fills the rest of the confining region. Emission from the filament is then space-charge limited such that $I_{emission}$ equals the loss rate of electrons from the confining region. As described in Sec. IV A 1, for experiments in CNT, the measurement of $I_{emission}$ can be used to find the average confinement time of electrons. For experiments that employ an injection method where not all of the emitted electrons enter the confining region, the emission current cannot be directly related to the confinement time. In those experiments, the confinement time is typically measured through the decay rate of image charge on a capacitive probe placed outside the plasma.[9–11,21]

The emitter filament is mounted near the end of a hollow 0.5 in. diameter ceramic rod. To maximize the number of surfaces that electrons have to cross to escape the confining region and hence maximize the confinement time, the rod is positioned so that the emitting filament resides on or near the magnetic axis.

C. The probes

The probes used to diagnose the plasma are filaments similar to the emitter filament—all are 10 W halogen light bulbs with the bulb glass removed, and all have the same dimensions d and L as the emitter filament. When cold, these filaments can only collect electrons and therefore behave as Langmuir probes. When heated sufficiently, the filaments can thermionically emit electrons. Whether a filament is a net source or net sink of electrons depends on $V_{probe} - \phi_p$ and the plasma temperature. Here V_{probe} is the probe potential and ϕ_p is the local plasma potential. Eight such filaments are mounted with equal spacing along a second rod positioned radially across the confining region. This allows for radial potential, density, and temperature measurements to be conducted without changing the rod's position. The third probe from the magnetic axis has been known to give unphysical measurements. The reason for this is presently unknown. Data from this probe is therefore omitted from this article. The eight filaments on this second rod are slightly different in that a 4 V battery is used to produce enough heating current to emit electrons while a 6 V battery is needed on the emitter. This is because the emitter filament is rated for 12 V while the probe filaments are all rated for 6 V. In both cases, they sufficiently thermionically emit at much less than their rated voltage.

D. The measurement electronics

Measurements in CNT require the simultaneous measurement of the current to and potential of a biased filament. A schematic of the circuit used to make these measurements is shown in Fig. 2. As shown in this figure, the filament potential is measured on a 100/1 voltage divider with $R_1 = 100\ \text{k}\Omega$ and $R_2 = 1\ \text{k}\Omega$ so that $V_{out} = V_{filament}/101$. The value of R_1 is chosen to be small enough to provide a good time response and large enough to stay below the maximum allowable current of the biasing power supply. The current is measured as the voltage across a resistor R_3 which is in series with the power supply and the plasma. For the emitter filament, $R_3 = 20\ \text{k}\Omega$, and for a probe filament, $R_3 = 1\ \text{M}\Omega$. A measurement of a few volts on the common-mode potential of the probe, typically hundreds of volts, is required. Because the common-mode of potential of the probe is only known to within a volt or two (the error of the measurement of the potential via the 100/1 voltage divider) the voltage drop across R_3 is measured directly. An isolation amplifier is used to translate the voltage across R_3 referenced to ground instead of the large common-mode potential. Floating poten-

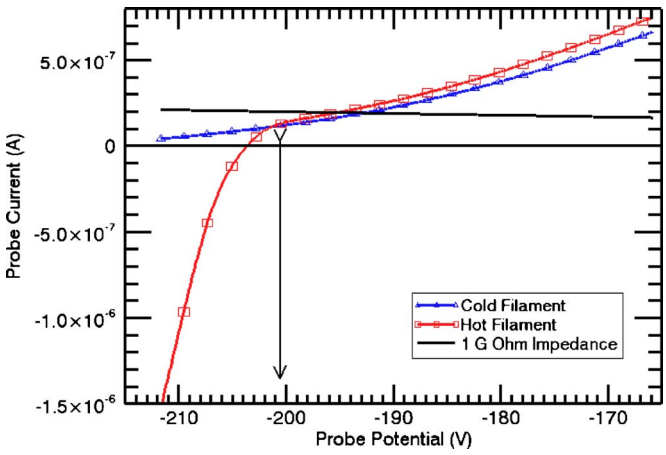

FIG. 3. (Color online) Hot (emissive) and cold (Langmuir) filament *IV* characteristics are shown in red and blue, respectively, for a pure-electron plasma in CNT with $B=0.02$ T, an emitter bias of $V_{\text{emitter}}=-200$ V, and a neutral pressure of $p_n=2\times10^{-8}$ Torr. The deviation potential is indicated by the potential where the trends in the hot and cold characteristics deviate. This appears at approximately −200.5 V in this figure. A 1 GΩ probe impedances shown as a black line having a slope corresponding to $V_{\text{probe}}/I_{\text{probe}}=1$ GΩ . The floating potential will occur at the potential where this probe impedance line intersects the *I-V* characteristic. This occurs at approximately −195 V for both characteristics and the 1 GΩ probe shown in this figure.

tial measurements, as described in detail in Sec. III A 2, are also performed using a 100/1 voltage divider but with $R_1=1$ GΩ and $R_2=10$ MΩ.

Additionally, large output impedances on V_{out} and I_{out} typically require additional buffer amplifiers to provide sufficient current for measurement. These are not shown in Fig. 2.

III. BASIC PROBE THEORY

Measurement of plasma parameters through the use of probes is done by determining the relationship between the probe current, I_{probe}, and the probe potential V_{probe} for a particular value or range of values of current or voltage. Figure 3 contains measurements of the hot (emissive) and cold (Langmuir) filament current-voltage (*I-V*) characteristics near the local plasma potential ϕ_p at the filament. As shown in this figure, for V_{probe} less negative than ϕ_p, both the cold and hot filaments collect electrons and the *I-V* characteristics are nearly identical. The difference between the hot and cold filament *I-V* characteristics shown in this figure are presumably caused by the finite voltage drop across the hot filament needed for heating and the finite size of the filament. A cold filament can only collect electrons so that as V_{probe} becomes more negative, I_{probe} asymptotically approaches zero current but never crosses it. On the other hand, a hot filament can emit electrons so that as V_{probe} becomes more negative the *I-V* characteristic of the hot filament deviates from the cold filament characteristic. As V_{probe} becomes even more negative, I_{probe} crosses zero and then the filament starts to emit a net current of electrons.

The remainder of this section describes how to interpret these measurements to determine plasma potential, density, and temperature.

A. Plasma potential

In pure-electron plasmas, ϕ_p is determined using two methods—the deviation potential ϕ_{dev} and the floating potential ϕ_f. The deviation potential is the more accurate of the two and can be used regardless of plasma temperature or density. However, measurements are more tedious, and information about the dynamics of the plasma potential cannot be determined with this method. The floating potential is the common method of measurement for plasma potential in pure-electron plasmas. It is less accurate than the deviation potential, and it cannot be measured in a low density plasma. The floating potential does, however, allow for dynamic measurement of potential making it useful even though it may lack accuracy. What follows is a description of the theory of these two techniques as applied to a pure-electron plasma.

1. The deviation potential

The so-called "deviation potential" is the potential at which hot filament and cold filament *I-V* characteristics deviate. This is the potential at which a hot filament begins to emit electrons—V_{probe} is slightly more negative than the local ϕ_p. The ϕ_{dev}, and therefore ϕ_p, can be accurately determined through a comparison of the hot and cold *I-V* characteristics as is shown in Fig. 3. This is equivalent to the procedure used in neutral plasmas for finding the deviation potential. The only difference is the absence of ion-saturation current in a pure-electron plasma.

This method has been used to determine local plasma potential in quasineutral plasmas.[22–25] It can be used to measure plasma potentials at arbitrarily high or low temperatures or densities—even the vacuum potential can be measured with this method[26]; this method is especially useful in the low densities typical of pure-electron plasmas.

There are a couple of issues associated with the use of this method to determine the local plasma potential. First, as previously mentioned, there is a difference between the hot and cold filament characteristics which is presumably caused by the finite heating-voltage drop across the filament and the finite filament size. If ϕ_p is determined directly from where the two characteristics cross, a systematic error in the determination of ϕ_p can result. However, ϕ_p can often be determined from the emissive characteristic alone by locating the knee in the characteristic. The sharpness of the knee in the hot filament characteristic is determined by the plasma temperature so determining ϕ_p from the location of the knee in the hot filament characteristic alone is easier in a colder plasma. It is also possible to look for a sharp change in the gradient of the difference between the hot and cold curves. The location of this sharp change is localized to where the trends diverge, even in the midst of a more general difference between the two characteristics. A more considerable issue is that because *I-V* characteristics must be measured to determine the plasma potential, this method cannot be used to determine the dynamics of ϕ_p which occur on a time-scale faster than the *I-V* sweep measurement time. In CNT this time is typically 5–10 s, making the deviation potential only useful for measuring steady-state or time-averaged values of ϕ_p.

2. The floating potential

The floating potential ϕ_f for any probe is defined as the potential of a probe which collects no net current from a plasma. This is therefore the x intercept of a I-V characteristic plotted as in Fig. 3. In experiments, the actual measured floating potential is the potential of a high impedance ($R_{\text{probe}} \approx 10\ \text{M}\Omega - 1\ \text{G}\Omega$) probe in the plasma. The measured potential will occur at the intersection of the I-V characteristic with the probe impedance characteristic—a line having the slope $I_{\text{probe}}/V_{\text{probe}} = 1/R_{\text{probe}}$. For the characteristics shown in Fig. 3, a 1 GΩ filament will have $\phi_f \approx -195$ V if it is hot or cold. For a high enough probe impedance, ϕ_f would differ dramatically between the hot and cold filaments.

Dynamics having characteristic time scales slower than $R_{\text{probe}}C_{\text{probe}}$ will be observed in the floating potential signal. Here C_{probe} is the probe capacitance. Because the determination of ϕ_f requires no measurements of I-V characteristics, measurements of ϕ_f are much easier than those of the deviation potential. In addition, information about the dynamics of the plasma potential are included in the time dependent ϕ_f measurement.

In the past, pure-electron experiments have reported ϕ_f of a Langmuir probe (i.e., a nonemissive probe) as ϕ_p.[9–11] ϕ_f for a Langmuir probe is, however, a poor measure of ϕ_p. Because there is no ion-saturation current in a pure-electron plasma and a Langmuir probe cannot emit electrons, the Langmuir probe I-V characteristic has no x intercept and so the theoretical floating potential is not defined. This is seen in Fig. 3 as the asymptotic approach of the cold filament characteristic to zero current for large negative potentials. As described above, if a probe of finite probe impedance is inserted in the plasma, the measured value of ϕ_f will occur at the intersection of the probe impedance line with the filament I-V characteristic of the plasma. Because the Langmuir characteristic is smooth in the region of ϕ_p and asymptotically approaches $I_{\text{probe}} = 0$ for $V_{\text{probe}} \ll \phi_p$, ϕ_f is a strong function of probe impedance and is therefore not easily related to ϕ_p. To illustrate this point, it is worth noting that while $\phi_f = -195$ V for the 1 GΩ probe shown in Fig. 3, $\phi_f = -180$ V and $\phi_f = -215$ V for $R_{\text{probe}} = 500\ \text{M}\Omega$ and $R_{\text{probe}} = 10\ \text{G}\Omega$, respectively.

In contrast to a Langmuir probe, an emissive probe can emit electrons. Therefore, it has a clear x intercept and thus a clear theoretical floating potential. The behavior of floating emissive probes has been previously studied in pure-electron plasmas[27,28] and has been used as a measure of plasma potential routinely in quasineutral experiments and in some pure-electron experiments[13,14] including, as described below, CNT. A hot filament I-V characteristic from CNT is shown in Fig. 3. In this figure, $I_{\text{probe}} = 0$A at $V_{\text{probe}} \approx -204$ V. The floating potential in Fig. 3 is more negative than ϕ_p as determined by the deviation potential. In fact, for quasineutral plasmas, the floating potential of an emissive probe has been shown to be related to the plasma potential through the electron temperature T_e by $\phi_f = \phi_p - \alpha T_e/e$ with $\alpha \leq 1$.[29] Because of the much larger mobility of electrons, the emissive probe floating potential is primarily a balance between emitted and collected electrons, and the ion current is negligible. Therefore, this result is applicable to a pure-electron plasma.

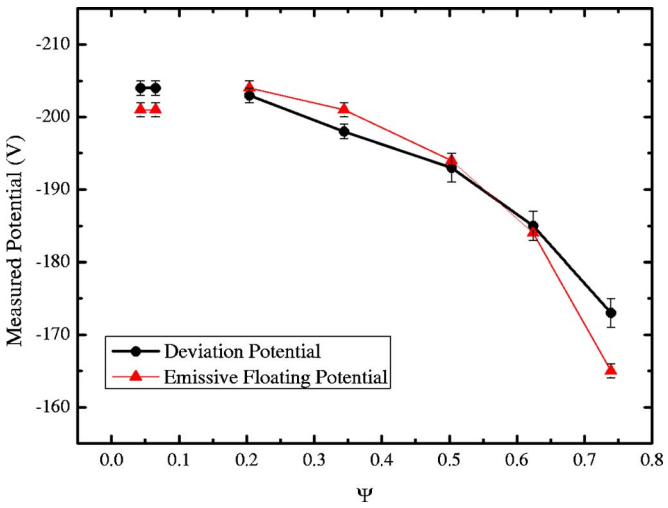

FIG. 4. (Color online) A comparison of the deviation potential and the floating potential profiles for $V_{\text{emitter}} = -200$ V, $B = 0.02$ T, and $p_n = 2 \times 10^{-8}$ Torr.

Because no I-V characteristics need to be measured, the measurement of ϕ_f is much easier than the measurement of the ϕ_{dev}. There are, however, two issues associated with using the floating potential of an emissive probe as a measure of the local plasma potential. First, increasing T_e broadens the emissive probe I-V characteristic in the knee region so that in hotter plasmas ϕ_f can differ significantly from ϕ_p. This manifests itself in the relation $\phi_f = \phi_p - \alpha T_e/e$ previously described. $\alpha \approx 1$, so without precise knowledge of T_e, ϕ_f of an emissive probe is a poor measure of ϕ_p in hot plasmas—plasmas with $T_e/e \gtrsim \phi_p$. Second, non-neutral plasmas typically have low densities and often have low cross field transport rates. In this situation, the plasma is unable to provide enough current for the probe potential to float near ϕ_p. This is the case for the plasma shown in Fig. 3; even a 1 GΩ impedance is insufficient to float the probe near the theoretical floating potential of $\phi_f = -204$ V. Without a dramatic increase in probe impedance, the absolute value of ϕ_f will be dependent on R_{probe}. For the hot filament I-V curve shown in Fig. 3, $R_{\text{probe}} \gtrsim 2\ \text{G}\Omega$ for $\phi_f < \phi_p$—the regime where ϕ_f is largely determined by ϕ_p and T_e instead of R_{probe}. The effect of insufficient density and probe impedance is also illustrated in Fig. 4. All probes for the measurements shown in this figure have $R_{\text{probe}} \approx 1\ \text{G}\Omega$. As described above, $\phi_{\text{dev}} = \phi_p$ while $\phi_f = \phi_p - \alpha T_e$. Therefore, $\phi_f = \phi_{\text{dev}} - \alpha T_e$ so that $\phi_f < \phi_{\text{dev}}$; for sufficient density and probe impedance, the floating potential is always more negative than the deviation potential. The density profile across the same region as the potential profiles shown in Fig. 4 is shown in Fig. 5. A comparison of the two figures indicates that for the plasmas shown in these figures, there is only sufficient density to float the probe for $\Psi \approx 0.2 - 0.5$. Here, Ψ is a coordinate that labels magnetic surfaces $\Psi = 0$ at the magnetic axis, and $\Psi = 1$ at the confining region edge. In the other regions the density and probe impedance are too low to properly float the probe potential.

In addition to producing an unreliable measurement, a probe with insufficient impedance may remove a significant portion of the electrons thereby resulting in an unacceptable

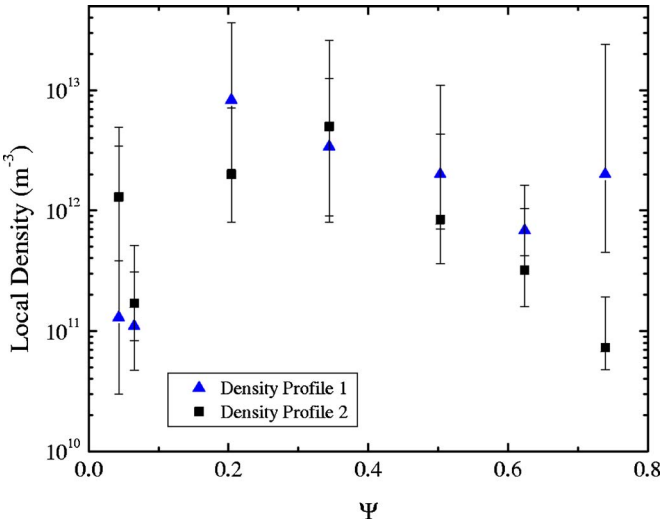

FIG. 5. (Color online) Two density profile measurements for $V_{\text{emitter}}=-200$ V, $B=0.02$ T, and $p_n=2\times10^{-8}$ Torr. "Density Profile 2" has been presented in a previously published article (Ref. 15). In both profiles, the density is peaked in the $\Psi\approx0.2-0.5$ region.

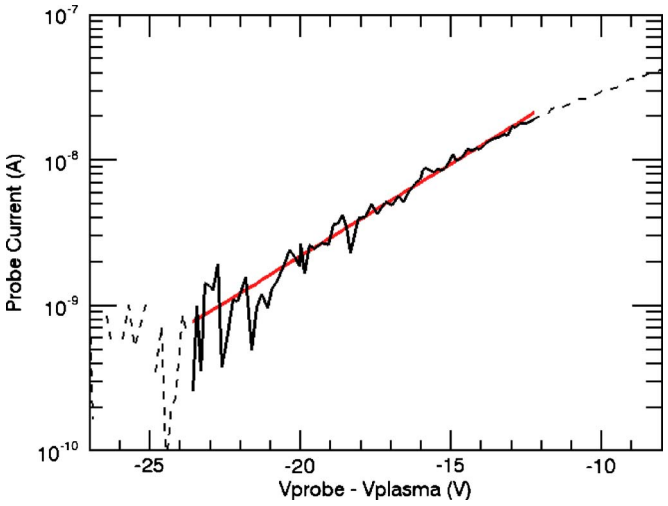

FIG. 6. (Color online) The dashed line is a Langmuir *I-V* characteristic (a cold probe) of the retarding region in a semilog I_{probe} vs $V_{\text{probe}}-\phi_p$ plot. A linear region of the characteristic is shown in solid black and a linear fit performed to this region is shown in red. For $V_{\text{probe}}-\phi_p<-24$ V, the probe current collected is buried in the signal noise. For $V_{\text{probe}}-\phi_p>-12$ V, the plasma is unable to supply electrons to the probe for the characteristic to be linear in this region and so the current rolls over for lower negative potential. The linear fit of $\ln(I_{\text{probe}})$ vs $V_{\text{probe}}-\phi_p$ in this region is used to determine both T_e and n_e.

perturbation. Increasing the probe impedance to much more than 1 GΩ is often fruitless because such impedances are on the same order as many of the insulating materials used in probe and electronics construction. Large impedances also tend to be significant sources of signal noise and limit the ability of the probe to react to the dynamics of the plasma. The use of large probe impedances, even if possible, may remove one of the main advantages of measuring the potential in this manner.

B. Electron temperature and density

As is often done in quasineutral plasmas,[30] the local electron temperature may be determined from the *I-V* characteristic of a Langmuir probe. In quasineutral plasmas the density is often determined through a measurement of the ion-saturation current.[30] The lack of ions makes such a measurement impossible in a pure-electron plasma. However, along with electron temperature, the electron density may also be determined from the *I-V* characteristic of a Langmuir probe. As described below, this method results in large uncertainties in the density measurements.

To determine temperature and density in a pure-electron plasma, the *I-V* characteristic is measured in the so-called retarding region of the characteristic—that region where the probe potential is more negative than the local plasma potential such that electrons must climb a potential hill to reach the probe. The electron current collected in the retarding region will be dependent on the distribution of velocities in the plasma. For a Maxwellian plasma, the density at the probe surface will be in a Boltzmann distribution: $n_{\text{probe}}=n_e e^{e(V_{\text{probe}}-\phi_p)/T_e}$, where n_e is the local electron density in the absence of the probe, e is the electron charge, and T_e is the local electron temperature. The collected current to the probe will then be

$$I_{\text{probe}}=\frac{1}{4}en_{\text{probe}}\bar{v}_eA=\frac{1}{4}en_e\bar{v}_eAe^{e(V_{\text{probe}}-\phi_p)/T_e}, \tag{1}$$

where e is the electron charge, $\bar{v}_e=\sqrt{2T_e/\pi m_e}$ is the mean Maxwellian velocity of electrons, and A is the probe collection area. A Maxwellian electron distribution will appear as an exponential region in the *I-V* characteristic. This exponential region will appear as a linear region in a plot of $\ln(I_{\text{probe}})$ vs $V_{\text{probe}}-\phi_p$ with a slope of $1/T_e$ in electron volts and a y intercept of $\ln(\frac{1}{4}en_e\bar{v}_eA)$. Therefore, the temperature is determined directly from the slope of the fit of this linear region, and the density can be determined from the y intercept as

$$n_e=\frac{4e^{y\text{ intercept}}}{e\bar{v}_eA}. \tag{2}$$

A semilog (I_{probe}) vs $V_{\text{probe}}-\phi_p$ plot of a cold filament *I-V* characteristic from CNT is shown in Fig. 6. Exponential amplification of uncertainties in the y intercept of the fit due to uncertainties in I_{offset} and ϕ_p cause large uncertainties in n_e. This is discussed in Sec. IV A 3.

Electron plasmas in CNT have $r_L\ll L_{\text{probe}}$, where r_L is electron cyclotron radius $r_L=m_e v_\perp/eB$. In this regime, the electrons are considered magnetized so that collection to the probe will occur only along field lines which intersect the probe. The collection area A of the probe must be estimated as the projection of these intersecting field lines on the probe surface.[30] For probe surfaces which are not spherical, this is at least partly dependent on the orientation of the probe relative to the field lines. Uncertainty in A should be considered in the uncertainty estimation of the electron density.

The densities associated with non-neutral plasmas are typically many orders of magnitude lower than those of quasineutral plasmas. There are complexities in these measurements which result from the low densities of pure-

electron plasmas. As previously mentioned, low densities limit the probe current available for measurement—even small currents may result in a substantial perturbation to the plasma. Measurements must therefore be made using probe currents as low as 10^{-9} A which can be quite difficult. In configurations such as CNT, which have long particle confinement times, the resulting low cross field transport rate further complicates measurements. Though particles travel very quickly along the field lines ($\approx 10\ \mu$s) they travel across field lines at the much slower cross field transport timescale (>1 ms). For probe collection current sufficient for measurement, the field line may be depleted of electrons thereby resulting in a substantial perturbation and distorted measurement. This would appear as a flattening of the *I-V* characteristic in the semilogarithmic plot where the probe current is highest—at less negative potentials. The linear region occurs over a narrower voltage range for a plasma with the same density and temperature but lower cross field transport rates (higher confinement times). In CNT, confinement time increases with magnetic field and decreases with neutral pressure so measurement difficulty can therefore be reduced with a change in these parameters. These effects are more substantial in closed field line devices such as pure-toroidal or dipole traps. As described above, the presheath of the probe extends along the field lines which intersect the probes. In a magnetic surface device such as CNT, the field lines travel around toroidally an infinite number of times thereby allowing the presheath to extend a great distance along the field lines. This lessens the likelihood of field line depletion. In closed field line configurations such as pure-toroidal and dipole traps, the field lines only extend $2\pi R$ around toroidally, greatly limiting the length the presheath can extend along the field lines. In these configurations, electron depletion of the magnetic field lines is therefore a much more serious concern.

Another concern is even though these plasmas often have low temperatures, the low densities result in large Debye lengths. Because of finite plasma temperature, insulating structures will charge up more negatively than the local ϕ_p so there will be a sheath region around the insulating materials of the probe structures. λ_D in CNT is approximately 1.7 cm, which is larger than the dimensions of both the probe filament and the distance of the filament from insulating structures. Measurements are therefore conducted in at least some portion of the sheath of the insulating materials. Such effects add to the uncertainty of potential measurements and must be considered in the analysis as a possible source of systematic error.

Another complexity which should be considered when making measurements of pure-electron plasmas using flux probes is, due to the substantial space-charge of these plasmas, there is typically a large, bulk $E\times B$ flow present. Depending on the scale of this flow, the Debye length, the cross field transport rate, and the orientation of the probe relative to the flow, this may result in a substantial perturbation to the probe current measurements.[27] A systematic error in plasma potential and/or density may result. In CNT, a series of erroneous measurement have been attributed to this effect. Two probe arrays were constructed to make radial profile measurements. The direction of the magnetic field was reversed through a reversal in the polarity of all of the magnetic coil power supplies. This produced a reversal in the $E\times B$ flow direction. Measurements on one array differed dramatically with the polarity reversed while only a slight effect was seen on the other array. Measurements from the array which was sensitive to $E\times B$ flow direction were discarded.

IV. MEASUREMENTS IN CNT

What follows is a detailed description of measurement complexities and techniques employed in CNT. Other than emissive floating potential measurements performed in other experiments,[13,14] this is the first time that these methods have been employed in pure-electron plasmas.

A. Measurement procedure in CNT

Typical impedances of insulating materials used in probe and electronics construction are in the range $100\ \text{M}\Omega - 10\ \text{G}\Omega$. Even in the absence of a plasma, a background current through the insulating materials can be as large as $I_{\text{background}} \approx 10^{-8}$ A. Typical densities in CNT are $n_e \approx 10^{12}\ \text{m}^{-3}$ resulting in I_{probe} from the plasma $I_{\text{plasma}} \approx 10^{-7} - 10^{-9}$ A. For the typical $V_{\text{probe}} \approx -10^2$ V in CNT, $I_{\text{plasma}} \approx I_{\text{background}}$. In fact, for an appreciable amount of the retarding region of the characteristic $I_{\text{plasma}} < I_{\text{background}}$. $I_{\text{background}}$ must therefore be measured and removed from the *I-V* characteristics for measurements to be successful.

The background current issue has been addressed in CNT by using the following experimental procedure for measuring the *I-V* characteristics. CNT is, at modest magnetic field strengths, a steady-state device allowing extended measurements. The measurement of *I-V* characteristics is performed by applying a triangle wave of potential to the probe over the desired probe potential range. A typical measurement is conducted over 60 s or more with a probe sweep period of 10 s—six or more cycles are recorded for each measurement. For the first 30 s the emitter filament is biased but not heated so there is no plasma. In this region, $I_{\text{probe}} = I_{\text{background}}$. At $t = 30$ s, the emitter heating current is applied and left on for the remainder of the measurement. For $t \geq 30$ s, $I_{\text{probe}} = I_{\text{plasma}} + I_{\text{background}}$. To recover I_{plasma}, a single cycle of the current signal from before $t = 30$ s is subtracted from all of the cycles of the current signal after $t = 30$ s. The probe current and potential sweeps for a cold filament with a plasma having $\phi_p = -203$ V are shown in Fig. 7.

In CNT, $I_{\text{background}}$ has been measured and can be modeled as a $R_{\text{background}} \approx 1\ \text{G}\Omega$ resistor in parallel with a $C_{\text{background}} \approx 1$ nF capacitor. An additional method of removing the background current, other than the one described above, would be to calculate $I_{\text{background}}$ from the measured V_{probe} signal using measured values of $R_{\text{background}}$ and $C_{\text{background}}$ for each probe. There are two problems associated with this method. The resulting currents from the plasma are small so errors in the determination of $I_{\text{background}}$ will have large effects on the measurements. Measurements would therefore be extremely sensitive to changes in the calibration of $R_{\text{background}}$ and $C_{\text{background}}$. The second problem is that noise in V_{probe} is amplified by a dV_{probe}/dt term in the calcu-

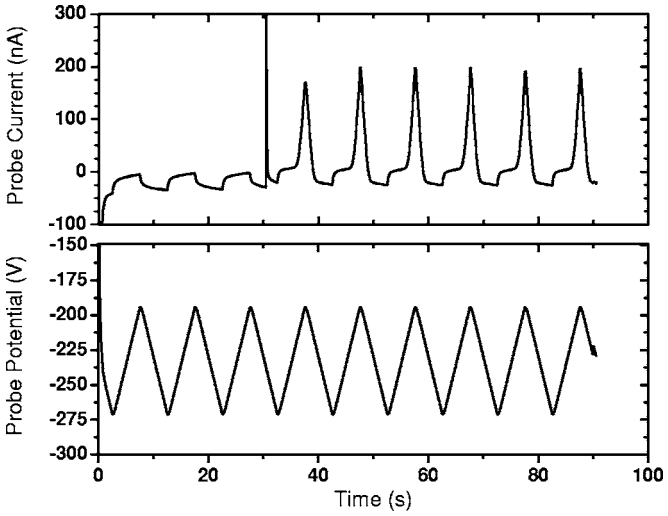

FIG. 7. The probe sweeping potential (bottom) and the current to the probe (top) for a cold filament at a local plasma potential of −203 V, $B=0.02$ T, and $p_n=2\times10^{-8}$ Torr. Plasma is introduced at $t=30$ s causing a spike in the current signal. The nonzero current signal which occurs previous to the introduction of the plasma is $I_{\text{background}}$. The lack of triangular form in $I_{\text{background}}$ is an indication of the nonzero capacitance in the probe and electronics.

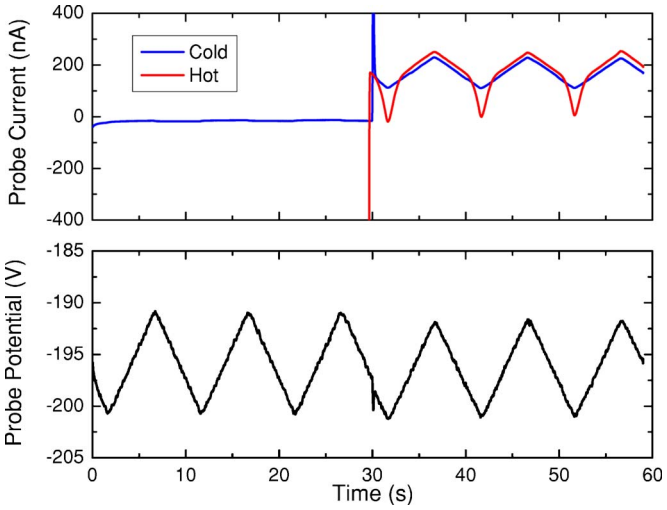

FIG. 8. (Color online) The probe sweeping potential (bottom) and the current to the probe (top) for a cold filament (blue) and a hot filament (red). $V_{\text{emitter}}=-200$ V, $B=0.02$ T, and $p_n=2\times10^{-8}$ Torr. The local ϕ_p for this filament is −198 V. The indication that the sweeping potential spans ϕ_p is seen in a bend in the otherwise triangular hot filament current signal. In this figure, this occurs when $I_{\text{probe}}\approx175$ nA.

lation of I_{probe}. Direct measurement and simple subtraction of $I_{\text{background}}$ for each measurement does not rely on any calibration other than the one required for measurement, and there is no amplification of noise. However, if the device is pulsed such that the *I-V* characteristic must be assembled from a series of separate measurements, the only way to address the background issue may be to calibrate, model, and subtract it.

For a particular set of experimental parameters (magnetic field strength, emitter bias, neutral pressure, etc.), the equilibrium is characterized by measurements of the plasma potential, density, and temperature profiles. This is done over the course of many separate measurements. The emission current of the negatively biased emitter filament is generally measured once for each set of experimental parameters so that the confinement time can be determined. To construct the profiles, the potential, density, and temperature are then measured on each of the probe filaments. The emission current and floating potentials on at least two of the available filaments are measured during any of these measurements. Any changes in equilibrium, including instabilities or large perturbations resulting from the probe potential sweep, will appear in these signals. The sweeping potential signals are chosen to make measurements without causing large perturbations to the equilibrium. The hot filament characteristics must not be swept much more negative than the local plasma potential or the filament will behave as a large source for electrons, possibly dwarfing the main emitter. The voltage on a filament must be negative enough (roughly as negative as the plasma potential) so it does not collect enough electrons to deplete the field lines which intersect the probe.

1. Confinement time

For a particular configuration and set of experimental parameters, the first measurement is typically the steady-state emission current I_{emission} of the negatively biased emitter filament. The measurement is performed by applying the bias to the filament without heating, and then applying the heating. The measured current when the filament is cold is subtracted from when the filament is hot to obtain I_{emission}. The total number of electrons confined N_e can be estimated from the subsequent measurement of the potential profile[20] or the equilibrium reconstruction using the density and temperature profiles.[15] The average electron confinement time is then determined through $\tau_c\approx eN_e/I_{\text{emission}}$, where e is the electron charge. During these measurements, all of the diagnostic filaments are heated and floating. ϕ_f is measured on the outer filament(s) such that fluctuations in ϕ_f, along with those in I_{emission}, indicate the presence of possible instabilities.

2. Potential measurements

The measurement of the local plasma potential at each filament is not only used to construct a plasma potential profile, but it is also used in the density and temperature measurements. To determine the local plasma potential the measurement of the hot filament characteristic and cold characteristic near ϕ_p over a probe potential range of 10 V is required. Because measuring ϕ_p requires sweeping V_{probe} through ϕ_p without knowing what ϕ_p is, finding ϕ_p is largely a matter of trial-and-error. The hot filament characteristic is measured so that the potential is swept slightly more negative than an educated guess for ϕ_p. A knee in the hot filament characteristic will be seen if the probe potential is swept through ϕ_p. The potential sweeping range is adjusted and repeated until this knee is seen near the most negative portion of the probe potential sweep; this will ensure minimal perturbation to the equilibrium during the measurement. The cold filament characteristic is then measured over this same range. Figure 8 shows hot and cold probe potential sweeps used to determine ϕ_p. The knee is the sharp bend in the otherwise triangular form of the hot filament current signal.

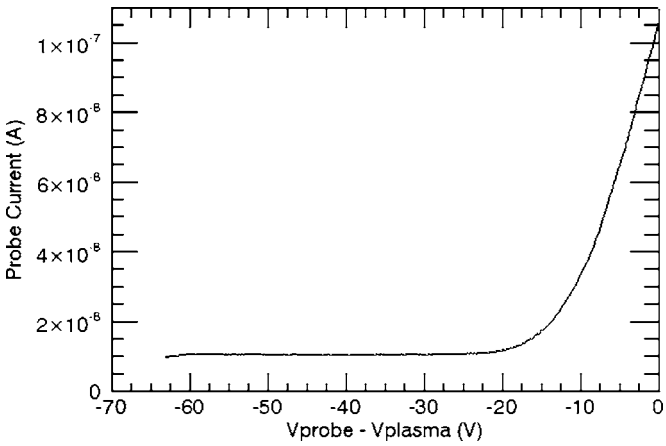

FIG. 9. A single sweep of Langmuir probe characteristic measurement shown in Fig. 7 after $I_{\text{background}}$ has been subtracted.

The probe potential sweeps involved in measuring ϕ_p result in larger currents than those used in the measurement of density and temperature. $I_{\text{background}}$ is therefore not as much of an issue as it is with the large negative potential sweeps required for the density and temperature measurements. The subtraction of this current from the characteristics generally has little effect on the measured value of ϕ_p.

It should be noted that in CNT, differences between the cold and hot filament characteristics for $V_{\text{probe}} > \phi_p$ are sometimes seen which are too large to be explained by the finite heating voltage on the hot filament. In these cases, the hot filament characteristic for $V_{\text{probe}} > \phi_p$ have an offset in current from measurement to measurement. The cause of this occasional offset is presently unknown. It does not, however, have an effect on the measurement of ϕ_p because the location of the knee which can be used to determine ϕ_p in the hot filament characteristic does not change even as the magnitude of the current offset does.

A measurement of the plasma potential profile is shown in Fig. 4. Typical errors for deviation potential measurements in CNT are 1%–2%.

3. Temperature and density measurements

Density and temperature measurements are performed by sweeping the potential of a cold filament over the range $V_{\text{probe}} \approx \phi_p$ to $V_{\text{probe}} \approx \phi_p - 100$ V. The current and voltage signals for such a measurement are shown in Fig. 7. As is described above, a full cycle of the $I_{\text{background}}$ is subtracted from all of the full cycles of $I_{\text{plasma}} + I_{\text{background}}$. Once this subtraction has been performed, each half-cycle is then analyzed as a separate *I-V* characteristic. Of course the experiments are steady state so each should, in principle, be the same. A single such half-cycle *I-V* characteristic is shown in Fig. 9. The collected electron current is expected to approach zero for large negative probe potentials, however, a measurable current offset I_{offset} often remains. In the case of the characteristic shown in Fig. 9, this offset is approximately 10 nA. It is thought that the source of this offset is the electronics, but, regardless, it should be subtracted from the whole characteristic before further analysis is performed. Uncertainty in the value of this offset is the main source of error in the measurements of density and temperature from the characteristic. Uncertainty in plasma potential, temperature, and probe area also contribute to the error in density but to a lesser degree. Each of the half-cycle *I-V* characteristics is viewed as a separate measurement of temperature and density. Analysis is performed separately on each one. The results are then combined into best values for density and temperature with error estimation. A set of algorithms was written into a computational routine to automate the density and temperature estimation and minimize any human bias in the results. What follows is a description of this set of algorithms.

For each of the half-cycle cold filament *I-V* characteristics like the one shown in Fig. 9, I_{offset}, the uncertainty in I_{offset}, and the level of noise in the characteristic are determined. I_{offset} is then subtracted from the signal. The dashed line in Fig. 6 is the semilog plot of the characteristic shown in Fig. 9 after this offset has been removed. To estimate a best-value for density and temperature and the uncertainties in each, a Monte Carlo routine is employed. A large (typically 100) number of characteristics are computationally generated from the original half-cycle characteristic by adding random values of a current offset, a potential offset, and noise having the same scale of I_{offset}, ϕ_p, and the signal noise, respectively. For each of these characteristics, the exponential region is found, a linear fit is performed on $\ln(I)$ in this region, and the temperature and density are calculated from the slope and y intercept while a figure of merit which involves the width of the fitting region and the quality of the fit is also calculated. The best temperature and density measurements are calculated as the figure-of-merit weighted average temperature and density from all of the characteristics. The distribution of temperature and density measurements about the best measurements is used to calculate the positive and negative uncertainties for these best measurements. The best values and uncertainties for each half-cycle characteristic are then combined as separate measurements into a single measurement of temperature and density with their respective uncertainties.

Typical measurements of temperature and density profiles are shown in Figs. 10 and 5, respectively. As indicated in these figures, the typical error for temperature measurements in CNT is 20%–30% while density measurements have much larger error bars.

V. SUMMARY

The characterization of the equilibrium of pure-electron plasmas in CNT involves the measurement of plasma potential, density, and temperature profiles. These measurements have been accomplished with an array of tungsten filaments which behave as emissive probes when sufficiently heated and Langmuir probes when cold. The local plasma potential is measured as the potential where the *I-V* characteristics of a filament, when hot and cold, deviate. The local temperature and density are determined through a measurement and interpretation of a series of cold filament *I-V* characteristics in the retarding region. The interpretation of these characteristics and the error propagation is conducted by a Monte Carlo routine which separately analyzes each characteristic and

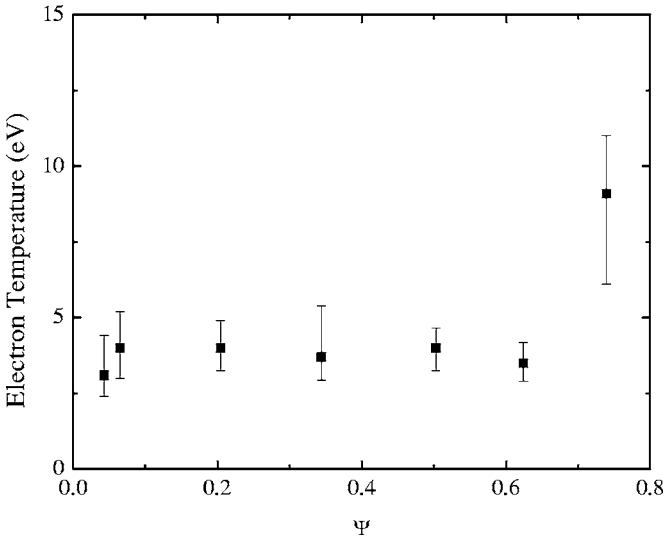

FIG. 10. A temperature profile measurement corresponding to the potential profile measurements shown in Fig. 4 and the density measurements shown in Fig. 5.

compiles the results into a single best-estimate for temperature and density with error estimates for each.

Measurements are complicated by the low densities and large $E \times B$ flows typical of pure-electron plasmas. The good confinement typical of an experiment like CNT complicates these measurements further. How these complications affect the measurements has been described in detail as were the measurement techniques developed to deal with these complications. The methods this article describes are easiest on a steady-state device, such as CNT, but, assuming reproducibility, these techniques may be applied to pulsed devices by combing measurements from several experiments.

The reader is referred to a previous publication[15] for results of pure-electron equilibrium experiments performed in CNT and analyzed using the techniques described in this article.

ACKNOWLEDGMENTS

The authors would like to acknowledge Jack Berkery for useful discussions. This work was supported by the United States DOE Grant No. DE-FG02–02ER54690 and by the NSF-DOE Partnership in Basic Plasma Science, Grant No. NSF-PHY-04–49813.

[1] R. C. Davidson, *Physics of Nonneutral Plasmas*, 2nd ed. (Imperial College Press and World Scientific Publishing, London, UK, 2001).
[2] J. H. Malmberg and J. S. deGrassie, Phys. Rev. Lett. **35**, 577 (1975).
[3] C. F. Driscoll, J. H. Malmberg, and K. S. Fine, Phys. Rev. Lett. **60**, 1290 (1988).
[4] M. R. Stoneking, M. A. Growdon, M. L. Milne, and R. T. Peterson, Phys. Rev. Lett. **92**, 095003 (2004).
[5] A. J. Theiss, R. A. Mahaffey, and A. W. Trivelpiece, Phys. Rev. Lett. **35**, 1436 (1975).
[6] E. P. Gilson and J. Fajans, Phys. Rev. Lett. **90**, 015001 (2003).
[7] J. H. Malmberg and C. F. Driscoll, Phys. Rev. Lett. **44**, 654 (1980).
[8] D. L. Eggleston, C. F. Driscoll, B. R. Beck, A. W. Hyatt, and J. H. Malmberg, Phys. Fluids B **4**, 3432 (1992).
[9] J. D. Daugherty, J. E. Eninger, and G. S. Janes, Phys. Fluids **12**, 2677 (1969).
[10] W. Clark, P. Korn, A. Mondelli, and N. Rostoker, Phys. Rev. Lett. **37**, 592 (1976).
[11] P. Zaveri, P. I. John, K. Avinash, and P. K. Kaw, Phys. Rev. Lett. **68**, 3295 (1992).
[12] T. S. Pedersen and A. H. Boozer, Phys. Rev. Lett. **88**, 205002 (2002).
[13] H. Saitoh, Z. Yoshida, C. Nakashima, H. Himura, J. Morikawa, and M. Fukao, Phys. Rev. Lett. **92**, 255005 (2004).
[14] H. Himura, Z. Yoshida, M. Isobe, S. Okamura, C. Suzuki, S. Nishimura, K. Matsuoka, K. Joi, and H. Yamada, Phys. Plasmas **11**, 492 (2004).
[15] J. P. Kremer, T. S. Pedersen, R. G. Lefrancois, and Q. Marksteiner, Phys. Rev. Lett. **97**, 095003 (2006).
[16] A. H. Boozer, Phys. Plasmas **5**, 1647 (1998).
[17] A. H. Boozer, Rev. Mod. Phys. **76**, 1071 (2005).
[18] T. Sunn Pedersen, A. H. Boozer, J. P. Kremer, W. T. Reiersen, F. Dahlgren, and N. Pomphrey, Fusion Sci. Technol. **46**, 200 (2004).
[19] T. Sunn Pedersen, J. P. Kremer, R. G. Lefrancois, Q. Marksteiner, X. Sarasola, and N. Ahmed, Phys. Plasmas **13**, 012502 (2006).
[20] T. Sunn Pedersen, J. P. Kremer, R. G. Lefrancois, Q. Marksteiner, N. Pomphrey, W. Reiersen, F. Dahlgren, and X. Sarasola, Fusion Sci. Technol. **50**, 372 (2006b).
[21] H. Saitoh, Z. Yoshida, and S. Watanabe, Phys. Plasmas **12**, 092102 (2005).
[22] F. F. Chen, in *Plasma Diagnostics Techniques*, edited by R. H. Huddlestone and S. I. Leonard (Academic, New York, 1965), p. 184.
[23] N. Hershkowitz and M. Cho, J. Vac. Sci. Technol. A **6**, 2054 (1988).
[24] J. R. Smith, N. Hershkowitz, and P. Coakley, Rev. Sci. Instrum. **50**, 210 (1979).
[25] W. E. Yao, T. Intrator, N. Hershkowitz, Rev. Sci. Instrum. **56**, 519 (1985).
[26] M. H. Cho, C. Chan, N. Hershkowitz, and T. I. Intrator, Rev. Sci. Instrum. **55**, 631 (1984).
[27] H. Himura, C. Nakashima, H. Saitoh, and Z. Yoshida, Phys. Plasmas **8**, 4651 (2001).
[28] H. Himura, M. Fukao, H. Wakabayashi, and Z. Yoshida, Rev. Sci. Instrum. **74**, 4658 (2003).
[29] M. Y. Ye and S. Takamura, Phys. Plasmas **7**, 3457 (2000).
[30] I. H. Hutchinson, *Principles of Plasma Diagnostics*, 2nd ed. (Cambridge University Press, Cambridge, UK, 2002).